Aftershocks resulting from creeping sections in a heterogeneous fault

G. Zöller,[1] S. Hainzl,[2] M. Holschneider,[3] and Y. Ben-Zion[4]

Received 29 October 2004; revised 6 January 2005; accepted 11 January 2005; published 10 February 2005.

[1] We show that realistic aftershock sequences with space-time characteristics compatible with observations are generated by a model consisting of brittle fault segments separated by creeping zones. The dynamics of the brittle regions is governed by static/kinetic friction, 3D elastic stress transfer and small creep deformation. The creeping parts are characterized by high ongoing creep velocities. These regions store stress during earthquake failures and then release it in the interseismic periods. The resulting postseismic deformation leads to aftershock sequences following the modified Omori law. The ratio of creep coefficients in the brittle and creeping sections determines the duration of the postseismic transients and the exponent p of the modified Omori law. **Citation:** Zöller, G., S. Hainzl, M. Holschneider, and Y. Ben-Zion (2005), Aftershocks resulting from creeping sections in a heterogeneous fault, *Geophys. Res. Lett.*, *32*, L03308, doi:10.1029/2004GL021871.

1. Introduction

[2] The occurrence of aftershock sequences is one of the most general patterns of observed seismicity. The temporal decay rate $\dot{n}(t)$ of the number of aftershocks is found to follow the modified Omori law [*Omori*, 1894; *Utsu et al.*, 1995]

$$\dot{n}(t) = (c + t - t_M)^{-p}, \tag{1}$$

where t_M is the occurrence time of the mainshock and the exponent p is close to 1 for observed seismicity.

[3] Many models were used to explain the frequency-magnitude distribution of observed seismicity [e.g., *Burridge and Knopoff*, 1967; *Bak and Tang*, 1989; *Dahmen et al.*, 1998]. In these models dealing solely with coseismic stress transfers and tectonic loading, aftershocks are not observed, unless the stress transfer on the fault becomes very weak. However, in such a case, the p value of the Omori law is unrealistically low [*Hergarten and Neugebauer*, 2002].

[4] Various mechanisms were proposed to explain the generation of aftershock sequences. These include viscoelastic relaxation in the fault zone [*Dieterich*, 1972; *Hainzl et al.*, 1999], fault strengthening or weakening after a block slips [*Ito and Matsuzaki*, 1990], pore fluid flow [*Nur and Booker*, 1972], rate-state friction [*Dieterich*, 1994], and damage rheology [*Ben-Zion and Lyakhovsky*, 2003; *Shcherbakov and Turcotte*, 2004]. While these mechanisms are based on time-dependent processes, *Hainzl et al.* [2003] have shown that foreshocks and aftershocks can also be explained by spatial effects, namely a decrease of strength localized at the edges of the rupture area. Some of the proposed models are, however, conceptual and it remains an open question whether these mechanisms can explain detailed observations of space-time earthquake clustering in natural fault systems.

[5] Empirical observations show that aftershocks are concentrated near the margin of fault areas where large coseismic displacements occur [*Utsu*, 2002], and partly on adjacent segments. A full numerical treatment of systems of segmented faults with realistic stress transfer requires very large computational effort. In the present work, we overcome this difficulty by using a fault plane that is divided by near-vertical aseismic barriers into separate segments. The aseismic barriers can undergo postseismic creep deformation and thus transfer stress from one fault segment to another. The presence of coseismic, postseismic and interseismic creep is now commonly observed by means of InSAR and other geodetic measurements [e.g., *Lyons and Sandwell*, 2003]. Numerous studies show that fault segments, e.g., along the San Andreas fault, can store stress and remain locked for certain periods, while other less brittle segments undergo a steady creep deformation [*Bürgmann et al.*, 2000].

[6] The model used in the present work is based on earlier works of *Ben-Zion* [1996] and *Zöller et al.* [2004, 2005] with a heterogeneous strike-slip fault in an elastic half-space. Various model ingredients, including the laws for brittle and creep deformation, stress transfer, and boundary conditions, are compatible with empirical knowledge. The simulations cover hundreds of years and allow us to reproduce brittle deformation as well as postseismic and interseismic creep deformation. The results indicate that a spatially heterogeneous distribution of brittle and creeping fault sections leads to realistic aftershock sequences compatible with observed data. We note that the assumed creeping barriers provide an effective way of parameterizing macroscopically a variety of physical processes including viscous relaxation, fluid migration, rate-state friction and damage.

2. Model

[7] In the first part of this section, we give a brief summary of the employed fault model following *Ben-Zion* [1996] and *Zöller et al.* [2004, 2005]. In the second part, we describe how the assumed brittle and creep mechanisms are implemented.

2.1. Model Framework

[8] The model includes a strike-slip fault region of 70 km length and 17.5 km depth, covered by a computational grid,

[1]Institute of Physics and Institute of Mathematics, University of Potsdam, Potsdam, Germany.
[2]Institute of Earth Sciences, University of Potsdam, Potsdam, Germany.
[3]Institute of Mathematics, University of Potsdam, Potsdam, Germany.
[4]Department of Earth Sciences, University of Southern California, Los Angeles, USA.

0094-8276/05/2004GL021871$05.00

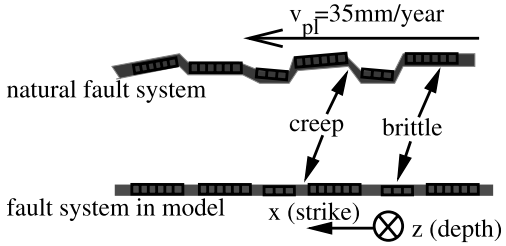

Figure 1. Sketch of a natural fault system and the linear approximation of the assumed fault model.

divided into 128 × 32 uniform cells, where deformational processes are calculated [*Ben-Zion and Rice*, 1993].

[9] Tectonic loading is imposed by a motion with constant velocity v_{pl} = 35 mm/year of the regions around the computational grid. The space-dependent loading rate provides realistic boundary conditions. Using the static stress transfer function for slip in elastic solid, the continuous tectonic loading for each cell on the computational grid is a linear function of time t. While the loading produces an increase of stress on the fault, the local stress may be reduced by creep and brittle failure processes.

[10] The ongoing creep motion on the computational grid is governed by a local constitutive law corresponding to lab-based dislocation creep. Specifically, we assume that the creep velocity is given by

$$\dot{u}_c(x,z;t) = c(x,z)(\tau(x,z;t))^3, \tag{2}$$

where x and z denote coordinates along strike and depth, $c(x, z)$ are time-independent coefficients, τ is the local stress and $\dot{u}$ is the creep velocity [*Ben-Zion*, 1996]. Equation (2) results in a system of 128 × 32 coupled ordinary differential equations, which is solved numerically using a Runge-Kutta scheme.

[11] An earthquake is initiated if the local stress $\tau(x, z; t)$ exceeds the static friction $\tau_s(x, z)$. Then the stress drops in cell (x, z) to the arrest stress $\tau_a(x, z)$ and the strength drops to a dynamic friction value $\tau_d(x, z)$ for the reminder of the event. At the end of the earthquake, the strength recovers back to the static level. The dynamic friction is calculated from the static and arrest stress levels in relation to a dynamic overshoot coefficient D:

$$\tau_d = \tau_s - \frac{\tau_s - \tau_a}{D}. \tag{3}$$

Following *Ben-Zion and Rice* [1993] and *Madariaga* [1976], we use D = 1.25. The static strength is constant, $\tau_s(x, z) \equiv 10$ MPa, and the arrest stress is chosen randomly from the interval $\tau_a(x, z) \in [0; 1$ MPa].

[12] The stress transfer due to coseismic slip and creep motion is calculated by means of the three-dimensional solution $K(x, z; x', z')$ of *Chinnery* [1963] for static dislocations on rectangular patches in an elastic Poisson solid with rigidity μ = 30 GPa:

$$\Delta\tau(x,z;t) = \sum_{(x',z')\in\text{fault}} K(x,z;x',z')\Delta u(x',z';t - r/v_s) \tag{4}$$

where Δu is the slip, r is the spatial distance between the cells (x, z) and (x', z'), v_s is a constant shear wave velocity, and the kernel K decays like $1/r^3$. The value of v_s defines the event time scale and has no influence on the earthquake catalogs. A finite value of v_s corresponds to the quasi-dynamic approximation of *Zöller et al.* [2004], whereas $v_s \to \infty$ reduces to the quasi-static procedure of *Ben-Zion and Rice* [1993] and *Ben-Zion* [1996]. The calculations below are done for a finite value of v_s, but the statistical aspects of the results remain the same for the quasi-static case.

2.2. Brittle and Creep Parameters

[13] Each cell of the computational grid is either a "brittle" or a "creep" cell. A brittle cell can undergo slip during an earthquake (coseismic) and small creep motion between two earthquakes (interseismic). A creep cell can only perform interseismic creep. Figure 1 shows a sketch of the distribution of brittle and creep cells. The creep barriers are generated by near-vertical random walks from various along-strike positions at the free surface to depth [*Ben-Zion*, 1996]. As shown below, the assumed barriers provide a simple way of simulating non-brittle deformation processes near segment boundaries (e.g., step-over regions) of a large strike-slip fault. The material surrounding the computational grid moves with a constant velocity v_{pl}. The model has two imposed timescales: A long time scale associated with the tectonic loading and a short earthquake timescale. In addition, there is a third emergent timescale generated by the interplay between the processes occurring on the brittle fault patches and creeping barriers.

[14] The creep coefficients for the brittle cells $c_b(x, z)$ in equation (2) are chosen similar to the values by *Ben-Zion* [1996] and *Zöller et al.* [2005]: $c_b(x, z)$ is randomly distributed in $[0.9\langle c_b\rangle;1.1\langle c_b\rangle]$, where $\langle c_b\rangle = 10^{-7}$ m s^{-1} MPa^{-3}. The coefficients for the creep cells $c_{cr}(x, z)$ are varied in different model simulations as follows: Model A: $\langle c_{cr}\rangle = 10^{-2}$ m s^{-1} MPa^{-3}, Model B: $\langle c_{cr}\rangle = 5 \cdot 10^{-3}$ m s^{-1} MPa^{-3}, and Model C: $\langle c_{cr}\rangle = 10^{-3}$ m s^{-1} MPa^{-3}. Noise is added to the mean values as for $c_b(x, z)$.

3. Model Simulations and Results

[15] For each model introduced at the end of the previous section, we perform a simulation with random initial stresses. After the stress field has reached a steady state, we produce an earthquake catalog containing 20,000 events and covering about 500 years. Figure 2 shows that the frequency-size distributions for all models include a scaling region followed by a characteristic earthquake at $M \approx 6.6$.

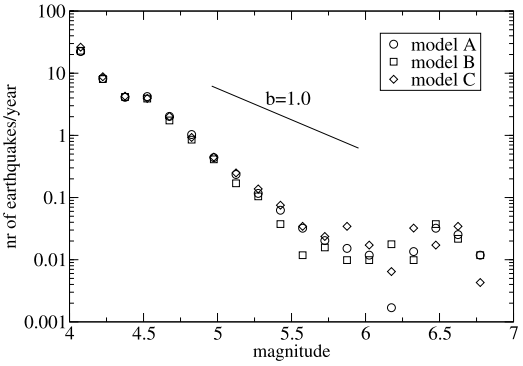

Figure 2. Frequency-size distributions for different model simulations.

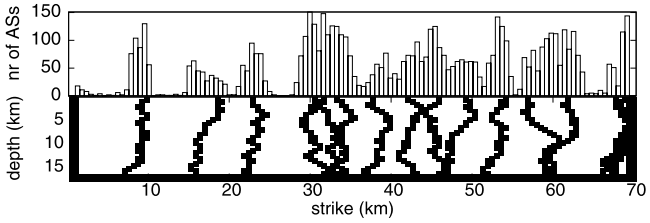

Figure 3. Model A: Hypocenter distribution of aftershocks (for a definition see text) along strike (top). Bottom: Distribution of brittle cells (white boxes) and creeping cells (black boxes) in the fault region.

Similar frequency-size distributions have been observed by *Ben-Zion* [1996] for a fault with uniform brittle properties. The fact that no earthquakes with $M < 4.0$ occur, stems from the discretization of the computational grid. Because the magnitude is derived from the cumulative slip during an event [*Ben-Zion*, 1996], the size of a cell determines the minimum magnitude. The bump at M = 4.5 is associated with the sizes of the brittle patches produced by the employed spatial realization of the creeping barriers.

[16] Figure 3 (bottom) shows the spatial distribution of creep and brittle cells in the fault region and the number of aftershocks along strike. Here, aftershocks are earthquakes occurring up to one year after a $M \geq 6.2$ mainshock. The aftershocks are mostly concentrated close to the near-vertical creep barriers (margins of the fault segments), which become highly loaded during mainshocks that transfer stress from the rupturing cells into the creeping parts of the fault. Because these parts do not fail in rapid brittle fashion, they store stress until each mainshock is terminated. After the mainshock they creep, thereby transferring stress back to the entire fault region. This leads to aftershocks, which occur preferentially close to creeping parts and in high stress fault patches that have not ruptured during the large event.

[17] Figure 4 (bottom) shows a typical aftershock sequence following a mainshock with magnitude $M = 6.6$. Immediately after the mainshock, the sequence is strongly clustered and becomes less concentrated some months later.

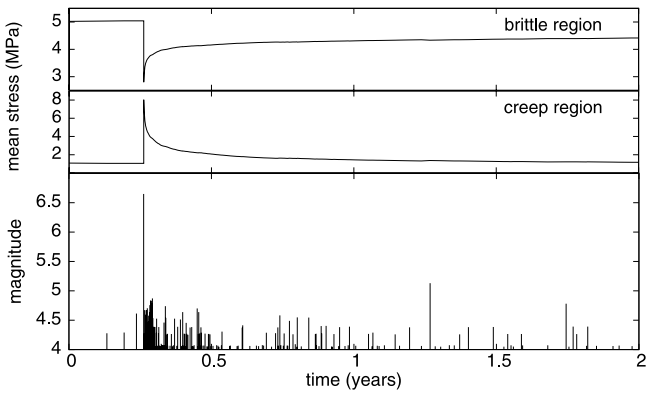

Figure 4. Example for a typical aftershock sequence in Model A: Mean stress as a function of time in the brittle region (top) and in the creeping region (middle panel) for a period of two years. The bottom panel shows earthquake magnitudes as a function of time.

The evolution of stress during this period in the brittle and creep regions is shown in the top and middle panel of Figure 4. The mean stress in the creeping regions grows rapidly during the occurrence of mainshocks and then relaxes. The mean stress in the brittle region drops at the time of the mainshock and then increases due to the stress transfer from the creeping cells. It is clear that the time scale of the stress relaxation in the creep regions depends on the average creep rate $\langle c_{cr} \rangle$. If this value grows, the creep velocity will increase according to equation (2). Thus, the relaxation becomes faster and aftershocks will occur in a shorter period after the main event. Comparing the bottom panel of Figure 4 with typical features of observed seismicity, we conclude that Model A represents a realistic scenario of aftershock activity.

[18] Figure 5 shows the mean earthquake rate after a mainshock in Models A, B, and C. The rate is stacked for all mainshocks with $M \geq 6.6$. The estimated p exponent of the modified Omori law and the level of background seismicity are indicated in each plot. The deviation of the aftershock activity from the background level can be measured by the ratio of earthquakes occurring up to three months after and before the main event. This ratio is about 10 for Models A and B, and about 6 for Model C. It is clearly visible that a high ratio of $\langle c_{cr} \rangle / \langle c_b \rangle$ (Model A) leads to aftershock sequences on short time scales characterized by relatively high exponents. A smaller ratio results in a slower stress transfer from creeping cells and thus leads to less clustered aftershock sequences (Model C). It is conspicuous that in Model C the maximum number of aftershocks is not observed directly after the mainshock. This is similar to the relative quiescence in the model without creep [*Ben-Zion and Rice*, 1993; *Zöller et al.*, 2004], which is due to the relative slow recovery of the stress field after the fault region has been unloaded by the mainshock. In particular,

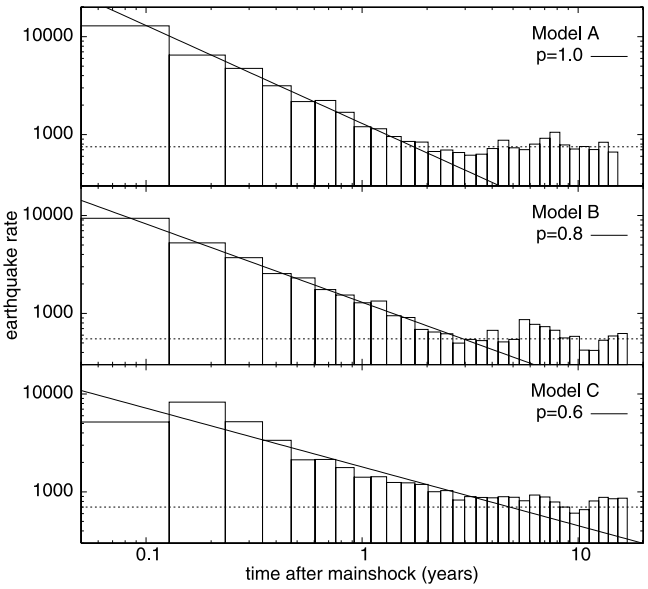

Figure 5. Earthquake rate as a function of time for different models. The solid lines give estimates of the modified Omori law and the dotted lines mark the background level of seismicity. Each plot is based on a simulation with 20,000 earthquakes covering about 500 years; the earthquake rates are averaged over about 30 mainshock cycles.

the amount of stress resulting from afterslip in Model C is too small to compensate the unloading of the fault due to the mainshock immediately after the mainshock. If the ratio $\langle c_{cr}\rangle/\langle c_b\rangle$ is close to 1, the loading of each brittle cell will be approximately linear. The results of Figure 5 indicate that Model A with $p = 1.0$ represents the most realistic case of aftershock sequences.

4. Discussion and Conclusions

[19] We study the behavior of a fault consisting of seismic segments separated by creeping regions that do not fail on the short earthquake timescale. Aseismic creep is known as an important process in fault zones [*Wesson*, 1988]. This is obvious for deep sections with ductile characteristics, but geodetic measurements as well as studies of seismic data indicate that creep plays also an important role in shallow parts of crust. It is interesting to note that the creep deformation of a fault may be of the same order of magnitude or even higher than the coseismic change. This has been observed, e.g., for the postseismic creep response of the 1984 Morgan Hill earthquake that occurred on the Calaveras fault in California [*Schaff et al.*, 1998].

[20] In our model, the interplay of brittle and creep deformation produces significant afterslip on creeping regions following large events. As a consequence, aftershocks are triggered on highly stressed fault patches that did not rupture during the mainshock. The occurrence of afterslip following large earthquakes has been documented in observational studies [e.g., *Bürgmann et al.*, 2002], and analyzed in laboratory experiments and numerical models [*Marone et al.*, 1991]. The p exponent of the modified Omori law and the time scale of aftershocks depend only on the coefficients of the imposed creep law (equation (2)). If the ratio of creep coefficients in the creeping and the brittle regions $\langle c_{cr}\rangle/\langle c_b\rangle$ is of the order 10^5, realistic aftershock sequences with $p \approx 1$ are observed. A study of foreshocks, which occur less frequent than aftershocks, requires a large number of mainshocks in various realizations. This is beyond the ability of our current computational method and is left for a future work.

[21] Summarizing, we have developed a fault model based on dislocation theory and empirical knowledge. The mixing of brittle and creep properties leads to postseismic effects, which are in agreement with numerous experiments and observational studies, and produce aftershock sequences following the modified Omori law. The high correspondence of the results to observations indicates that the model provides an effective parameterization of the key physical process that govern seismicity on large strike-slip faults.

[22] **Acknowledgments.** G. Z. acknowledges support from the collaborative research center "Complex Nonlinear Processes" (SFB555) of the German Research Society (DFG). We thank Ilya Zaliapin and anonymous reviewer for useful comments.

References

Bak, P., and C. Tang (1989), Earthquakes as a self-organized critical phenomenon, *Geophys. Res. Lett.*, *94*, 15,635–15,637.

Ben-Zion, Y. (1996), Stress, slip, and earthquakes in models of complex single-fault systems incorporating brittle and creep deformations, *J. Geophys. Res.*, *101*, 5677–5706.

Ben-Zion, Y., and V. Lyakhovsky (2003), A generalized law for aftershock rates in a damage rheology model, *Eos Trans. AGU*, *84*(46), Fall Meet. Suppl., Abstract NG12C-02.

Ben-Zion, Y., and J. R. Rice (1993), Earthquake failure sequences along a cellular fault zone in a three-dimensional elastic solid containing asperity and nonasperity regions, *J. Geophys. Res.*, *98*, 14,109–14,131.

Bürgmann, R., D. Schmidt, R. M. Nadeau, M. d'Alessio, E. Fielding, D. Manaker, T. V. McEvilly, and M. H. Murray (2000), Earthquake potential along the northern Hayward fault, California, *Science*, *289*, 1178–1182.

Bürgmann, R., S. Ergintav, P. Segall, E. H. Hearn, S. McClusky, R. E. Reilinger, H. Woith, and J. Zschau (2002), Time-dependent distributed afterslip on and deep below the Izmit earthquake rupture, *Bull. Seismol. Soc. Am.*, *92*, 126–137.

Burridge, R., and L. Knopoff (1967), Model and theoretical seismicity, *Bull. Seismol. Soc. Am.*, *57*, 341–371.

Chinnery, M. (1963), The stress changes that accompany strike-slip faulting, *Bull. Seismol. Soc. Am.*, *53*, 921–932.

Dahmen, K., D. Ertas, and Y. Ben-Zion (1998), Gutenberg-Richter and characteristic earthquake behavior in simple mean-field models of heterogeneous faults, *Phys. Rev. E*, *58*, 1494–1501.

Dieterich, J. H. (1972), Time-dependent friction as a possible mechanism for aftershocks, *J. Geophys. Res.*, *77*, 3771–3781.

Dieterich, J. H. (1994), A constitutive law for earthquake production and its application to earthquake clustering, *J. Geophys. Res.*, *99*, 2601–2618.

Hainzl, S., G. Zöller, and J. Kurths (1999), Similar power laws for fore- and aftershock sequences in a spring-block model for earthquakes, *J. Geophys. Res.*, *104*, 7243–7253.

Hainzl, S., G. Zöller, and F. Scherbaum (2003), Earthquake clusters resulting from delayed rupture propagation in finite fault segments, *J. Geophys. Res.*, *108*(B1), 2013, doi:10.1029/2001JB000610.

Hergarten, S., and H. J. Neugebauer (2002), Foreshocks and aftershocks in the Olami-Feder-Christensen model, *Phys. Rev. Lett.*, *88*, 238501, doi:10.1103/PhysRevLett.88.238501.

Ito, K., and M. Matsuzaki (1990), Earthquakes as self-organized critical phenomena, *J. Geophys. Res.*, *95*, 6853–6860.

Lyons, S., and D. Sandwell (2003), Fault creep along the southern San Andreas from interferometric synthetic aperture radar, permanent scatterers, and stacking, *J. Geophys. Res.*, *108*(B1), 2047, doi:10.1029/2002JB001831.

Madariaga, R. (1976), Dynamics of an expanding circular fault, *Bull. Seismol. Soc. Am.*, *66*, 639–666.

Marone, C. J., C. H. Scholz, and R. Bilham (1991), On the mechanisms of earthquake afterslip, *J. Geophys. Res.*, *96*, 8441–8452.

Nur, A., and J. R. Booker (1972), Aftershocks caused by pore fluid flow?, *Science*, *175*, 885–887.

Omori, F. (1894), On the aftershocks of earthquakes, *J. Coll. Sci. Imp. Univ. Tokyo*, *7*, 111–200.

Schaff, D. P., G. C. Beroza, and B. E. Shaw (1998), Postseismic response on repeating aftershocks, *Geophys. Res. Lett.*, *25*, 4549–4552.

Shcherbakov, R., and D. L. Turcotte (2004), A damage mechanics model for aftershocks, *Pure Appl. Geophys.*, *161*, 2379, doi:10.1007/s00024-004-2570-x.

Utsu, T. (2002), Statistical features of seismicity, in *International Handbook of Earthquake and Engineering Seismology, Int. Geophys. Ser.*, vol. 81A, edited by W. H. K. Lee et al., pp. 719–732, Elsevier, New York.

Utsu, T., Y. Ogata, and R. S. Matsu'ura (1995), The centenary of the Omori formula for a decay law of aftershock activity, *J. Phys. Earth*, *43*, 1–33.

Wesson, R. L. (1988), Dynamics of fault creep, *J. Geophys. Res.*, *93*, 8929–8951.

Zöller, G., M. Holschneider, and Y. Ben-Zion (2004), Quasi-static and quasi-dynamic modeling of earthquake failure at intermediate scales, *Pure Appl. Geophys.*, *161*, 2103, doi:10.1007/s00024-004-2551-0.

Zöller, G., M. Holschneider, and Y. Ben-Zion (2005), The role of heterogeneities as a tuning parameter of earthquake dynamics, *Pure Appl. Geophys.*, in press.

Y. Ben-Zion, Department of Earth Sciences, University of Southern California, Los Angeles, Los Angeles, CA 90089–0740, USA. (benzion@usc.edu)

S. Hainzl, Institute of Earth Sciences, University of Potsdam, POB 60 15 53, D-14415 Potsdam, Germany. (hainzl@geo.uni-potsdam.de)

M. Holschneider, Institute of Mathematics, University of Potsdam, POB 60 15 53, D-14415 Potsdam, Germany. (hols@math.uni-potsdam.de)

G. Zöller, Institute of Physics and Institute of Mathematics, University of Potsdam, POB 60 15 53, D-14415 Potsdam, Germany. (gert@agnld.uni-potsdam.de)